Journal of Power Sources 241 (2013) 589–596

Contents lists available at SciVerse ScienceDirect

Journal of Power Sources

journal homepage: www.elsevier.com/locate/jpowsour

Short communication

Application of poly (p-phenylene oxide) as blocking layer to reduce self-discharge in supercapacitors

Tete Tevi, Houman Yaghoubi, Jing Wang, Arash Takshi*

Department of Electrical Engineering, University of South Florida, Tampa, FL 33620, USA

HIGHLIGHTS

- We have studied the effect of a PPO layer on the characteristics of a supercapacitor.
- We have studied the thickness of a PPO layer using electrochemical impedance spectroscopy (EIS).
- Application of the blocking layer reduces the leakage current.
- Energy waste is lower in a supercapacitor with the blocking layer.
- Specific capacitance decreases in presence of the blocking layer.

ARTICLE INFO

Article history:
Received 18 January 2013
Received in revised form
28 April 2013
Accepted 29 April 2013
Available online 13 May 2013

Index terms:
Supercapacitors
Self-discharge
Leakage current
Electrodeposition
Poly (p-phenylene oxide) (PPO)

ABSTRACT

Supercapacitors are electrochemical energy storage devices with high power density. However, application of supercapacitors is limited mainly due to their high leakage current. In this work, application of an ultra-thin layer of electrodeposited poly (p-phenylene oxide) (PPO) has been investigated as a blocking layer to reduce the leakage current. The polymer was first deposited on a glassy carbon electrode. The morphology of the film was studied by atomic force microscopy (AFM), and the film thickness was estimated to be ~1.5 nm by using the electrochemical impedance spectroscopy (EIS) technique. The same deposition method was applied to coat the surface of the activated carbon electrodes of a supercapacitor with PPO. The specific capacitance, the leakage current, and the series resistance were measured in two devices with and without the blocking layer. The results demonstrate that the application of the PPO layer reduced the leakage current by ~78%. However, the specific capacitance was decreased by ~56%, when the blocking layer was applied. Due to the lower rate of self-discharge, the suggested approach can be applied to fabricate devices with longer charge storage time.

1. Introduction

Application of energy storage devices is growing rapidly due to the demand for more mobile and wireless electronics. Potentially, supercapacitors are suitable alternatives for batteries in applications, where high power density is needed (e.g. wireless devices and electric/hybrid vehicles) [1]. Also, supercapacitors have larger cycle lifetime than batteries. A supercapacitor can be charged and discharged up to a million times, whereas a typical rechargeable battery can be used up to only ~1000 cycles [2,3]. The large cycle lifetime is vital in small electronics which are designed to harvest energy from ambient sources. In fact, the market for wireless sensors equipped with energy harvesting units is growing rapidly for various applications such as structural health and traffic monitoring [4]. Despite the advantages, practically, the application of supercapacitors is very limited mainly due to high leakage current in the devices. The leakage current results in self-discharge effect in supercapacitors and inefficient charging/discharging cycles with energy waste during each cycle [3,5,6]. The leakage problem is more serious in devices powered by harvesting solar, thermal, or vibration energy. The amount of harvested power is usually very low (10–1000 μW [7]). Hence, the amount of current available for charging a supercapacitor is limited. If the current value is less than the leakage current, the supercapacitor cannot be charged at all. The leakage problem has been investigated extensively through modeling supercapacitors [8–11] and the electrochemical study of the electrode–electrolyte interface [12–14]. Yet no practical solution has been applied for decreasing the leakage current in supercapacitors. In this work, we have studied the

* Corresponding author.
E-mail addresses: tete@mail.usf.edu (T. Tevi), hyaghoubi@mail.usf.edu (H. Yaghoubi), jingw@usf.edu (J. Wang), atakshi@usf.edu, arash.takshi@gmail.com (A. Takshi).

0378-7753/$ – see front matter © 2013 Elsevier B.V. All rights reserved.
http://dx.doi.org/10.1016/j.jpowsour.2013.04.150

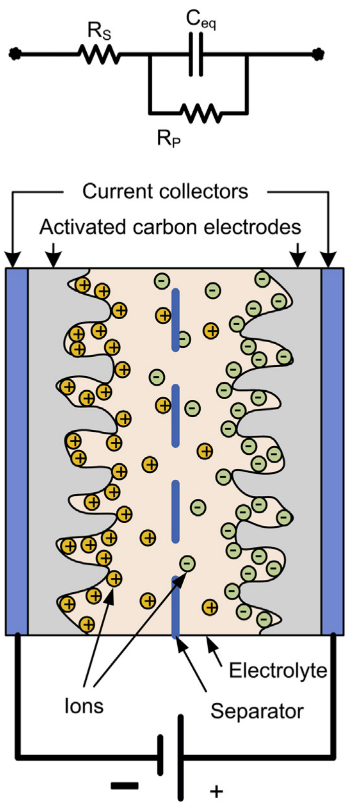

Fig. 1. A cross section view and a simplified model for a supercapacitor.

application of an ultra-thin insulating layer (blocking layer) between the electrode and the electrolyte as a potential solution for reducing the leakage current, particularly for wireless sensor applications.

The most popular form of a supercapacitor is the electrochemical double layer capacitor (EDLC) [2]. Fig. 1 shows the structure of an EDLC, which is made of two porous electrodes in an electrolyte. When a voltage is applied across the device (charging process), ions move from the bulk electrolyte toward the electrodes and form double layer charges (Fig. 2a). The double layer mimics a parallel plate capacitor with the solvent material as the dielectric, with permittivity of ε_S, between ionic and electronic charges. Due to the small distance between the opposite charges ('d' in Fig. 2a), the double layer capacitance ($C_{DL} = \varepsilon_S/d$) is typically in the range of 5–20 μF cm^{-2} [2]. To achieve high specific capacitance, C_{sp}, (capacitance per mass, F g^{-1}, or capacitance per volume, F cm^{-3}) in supercapacitors, porous electrodes with extremely large surface area are employed. The energy can be stored in EDLCs by charging the device. Similar to a capacitor, the energy density is equal to $0.5C_{sp}\,V^2$, where V is the applied charging voltage. Once the device is charged, the charge across the double layer has to be preserved to store the energy. However, as shown in Fig. 2a, a redox reaction (Faradic reaction) may occur at the electrode surface through which electrons pass through the double layer and discharge the capacitor. The effect of the Faradic reactions appears as the leakage current, which results in the self-discharge effect. As a solution, an ultra-thin layer of an insulating material can be employed on the electrode surface to block the electron transfer and reduce the leakage current (Fig. 2b).

For better understanding the effect of the leakage current, a supercapacitor can be modeled with an ideal capacitance, C_{eq}, a series resistance, R_S, and a parallel resistance, R_P (Fig. 1). Considering a double layer capacitor at each electrode, C_{eq} is the equivalent capacitance of both capacitors in series. R_S includes the contact and the electrolyte resistances, and R_P represents the leakage path. The main source of the leakage current is Faradic reactions at the electrode surface [13]. The amount of the leakage current is proportional to the reaction rate. The rate of the electron transfer depends on the reduction potential of the redox reaction, E_0, and the applied voltage, V, across the double layer. The difference between V and E_0 is known as the overpotential ($=V - E_0$). According to Tafel equation [15], the Faradic reaction rate is related exponentially to the overpotential, meaning that the leakage current increases exponentially with the increase in the applied voltage. Therefore, R_P is a function of the applied voltage with the lowest value when the device is charged up to the maximum voltage. As a result of the leakage, a typical device loses 10% of the stored energy in less than 1 h [16]. In practice, it is recommended to charge supercapacitors to the voltages lower than the nominal value for controlling the leakage current [17]. However, since the energy density is proportional to V^2, reducing the voltage decreases the amount of stored energy significantly and makes supercapacitors less efficient than batteries for applications with size constraint.

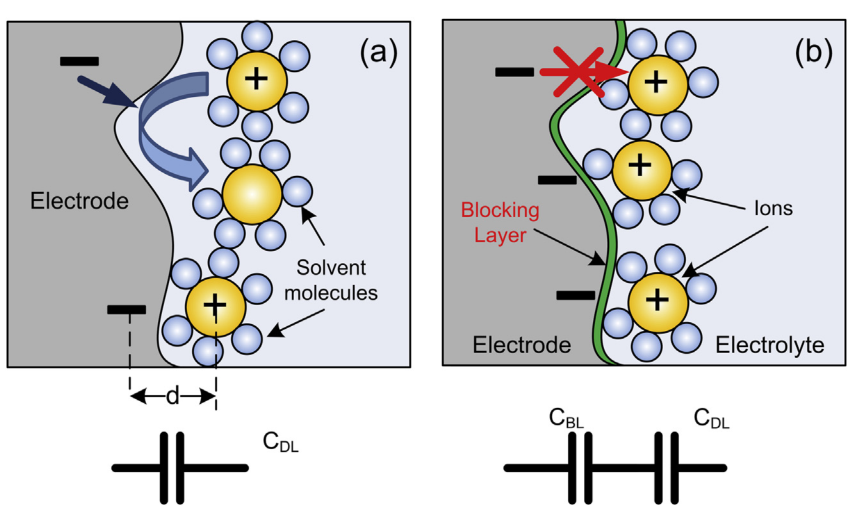

Fig. 2. Schematics of the electrode–electrolyte interface (double layer charges) in supercapacitors. The charge arrangement can be modeled with capacitors. (a) Electrochemical reaction at the surface of the electrode results in charge loss. (b) Application of a thin blocking layer decreases the reaction rate and enhances the energy storage capability.

The electrochemical reaction rate can be lowered by application of an insulating layer (blocking layer) on the electrodes. The effect of the blocking layer can be modeled as a capacitance, C_{BL}, in series with the double layer capacitance C_{DL} (Fig. 2b). It should be noted that the blocking layer is not hindering the double layer capacitance. The coating increases the distance between ionic and electronic charges and provides an energy barrier for Faradic reactions. Therefore, the equivalent capacitance is $C_{eq} = C_{BL}C_{DL}/(C_{BL} + C_{DL})$ which is always smaller than C_{DL}. In order to minimize the capacitance reduction, C_{BL} has to be much larger than C_{DL}. Due to the very small distance between negative and positive charges in a double layer capacitor, this can happen only if an ultrathin ($\sim$1 nm) high dielectric material is applied as the blocking layer. It is anticipated to have a C_{DL} in the same range of C_{BL} if a thin layer (1–2 nm) of an insulating polymer ($\varepsilon_r \approx 3.5$) is applied. In this case, C_{eq} would be about half of the double layer capacitance. The key point in minimizing the capacitance reduction is to deposit an ultrathin and uniform layer of the polymer on the electrodes. In this work, a thin layer of poly (p-phenylene oxide), PPO, on the electrodes was deposited, acting as the blocking layer. Electrodeposition is an easy method for coating conductive surfaces with conformal thin films [18]. It has been demonstrated that the electrodeposition of PPO can produce a pin-hole free thin-film layer on conductive substrates [19,20]. Ultra-thin PPO films are stable in organic and aqueous electrolytes, and do not block the formation of an electrical double layer, when deposited on conductive substrates [21]. The mechanism of deposition is based on polymerization of a monomer in an electrochemical reaction. Due to the low conductivity of PPO, the resistance of the polymer chain increases as the film grows. The high resistance leads to formation of a passivation layer, which stops the further growth of PPO. The self-limiting growth mechanism generates an ultra-thin film of PPO with a thickness of about a few nanometers [19]. Fig. 3 shows the phenol monomer and the PPO molecule after electropolymerization.

In order to study the morphology and measure the thickness of the blocking layer, a PPO layer was first deposited on a glassy carbon substrate (flat and smooth surface). Then surface coverage and roughness of the PPO layer were studied using atomic force microscopy (AFM), and the thickness was estimated from an electrochemical impedance spectroscopy (EIS) experiment. After that, the surface of two activated carbon electrodes was coated with a layer of PPO, and the electrodes were utilized to make a supercapacitor. Also, another capacitor was fabricated with no coating. C_{eq}, R_P and R_S were measured in both devices through electrochemical experiments, including cyclic voltammetry (CV), open circuit voltage measurement, and galvanic pulses. The difference between the parameters in both devices has been discussed, which indicates the effect of the blocking layer on the performance of a supercapacitor.

2. Experimental

The electrochemical experiments were performed using a VersaSTAT 4 (Princeton Applied Research) potentiostat. Activated carbon electrodes from Y-Carbon (www.y-carbon.us) and glassy carbons from SPI Supplies (www.2spi.com) were used as the electrodes. All the other chemicals were purchased from Sigma and used without further purification.

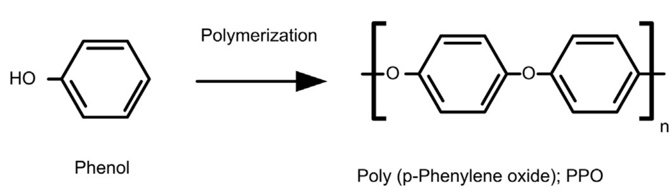

Fig. 3. Phenol monomer and PPO polymer.

2.1. PPO electrodeposition

The developed method explained by Rhodes et al., has been modified for PPO electrodeposition [19]. The phenylene oxide monomer solution was prepared with 50 mM tetramethylammonium hydroxide, 0.1 M tetrabutylammonium perchlorate, and 50 mM phenol solvated in propylene carbonate. The PPO deposition was performed in a three electrode cell configuration with Ag/AgCl reference electrode and a coiled Pt wire as the counter electrode. The working electrode was either a glassy carbon (area of $\sim$0.5 cm^2) or pieces of activated carbon each with apparent surface area of 0.5 cm^2. Cyclic voltammetry (CV) technique was applied for PPO deposition [19]. The working electrode potential was scanned for 22 cycles between −45 mV and +955 mV versus Ag/AgCl with the scan rate of 50 mV s^{-1}. After the electrodeposition, the electrodes were rinsed with propylene carbonate.

2.2. Atomic force microscopy (AFM)

The morphology of the glassy carbon electrode before and after PPO electrodeposition was studied with tapping mode AFM (Digital Instruments) in air. AFM probes with a resonant frequency of $\sim$300 kHz were employed in the measurements.

2.3. Electrochemical impedance spectroscopy (EIS)

EIS measurement was performed on the glassy carbon electrode before and after PPO deposition to investigate the effect on capacitance and leakage current, and measure the thickness of the blocking layer. The EIS tests were performed in three probe setup with Ag/AgCl reference and the Pt counter electrodes. The electrolyte was a solution of 1 M tetrabutylammonium hexafluorophosphate (TBAP) in propylene carbonate. The experiments were conducted in the range of 10 mHz–100 kHz with AC amplitude of 10 mV and DC bias of 0 V versus open circuit potential.

2.4. Device fabrication and characterization

For fabricating supercapacitors, two pieces of activated carbon, each with apparent surface area of 0.5 cm^2, were used. The glassy carbon electrodes were used as the back contact for current collection. A mesh of polyester was applied as a separator between the activated carbon electrodes. A custom-made Teflon screw-clamp was developed and used to press activated carbons to the back contact electrodes, while the electrodes were immersed into the electrolyte solution containing 1 M TBAP in propylene carbonate. A picture of the setup is shown in Fig. 4. To test the effect of the blocking layer, activated carbon electrodes with and without PPO deposited layer were tested. The devices were characterized by multiple cyclic voltammetry, open circuit self-discharge study, and galvanic pulses.

3. Results and discussion

3.1. PPO deposition and characterization

In order to gain high specific capacitance, porous electrodes are commonly employed to fabricate supercapacitors. However, studying the quality and estimating the thickness of the blocking layer on a porous electrode is challenging. Therefore, first we have deposited PPO on a smooth glassy carbon electrode. The blocking

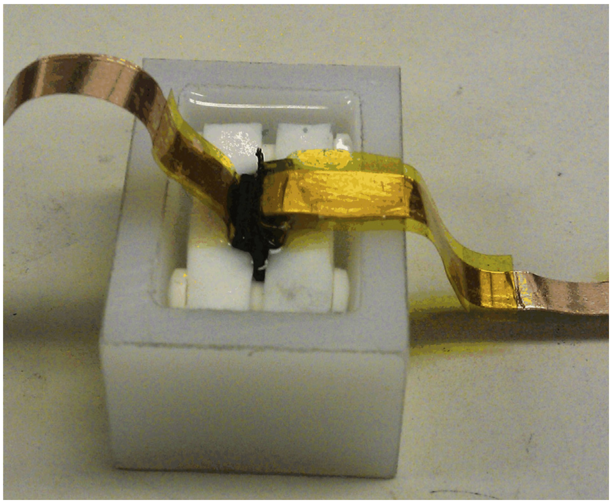

Fig. 4. A picture of the fabricated supercapacitor.

layer was deposited on the electrode by multiple cyclic voltammetry (CV) for 22 cycles (Fig. 5). The CV result is similar to the previous results reported by Rhodes et al. [19]. The current decrease in every cycle demonstrates the deposition of the PPO layer and the growth of the insulating layer [19,22,23]. The morphology of the glassy carbon electrode before and after PPO deposition was studied using AFM. As shown in Fig. 6, the morphologies were quite different. The surface of the glassy carbon electrode showed a smooth microstructure with root-mean-square (RMS) roughness of ~1.67 nm, while the roughness is increased to ~3.66 nm after the deposition (Fig. 6a and b). The electropolymerized PPO film showed a well-uniform coherent layer on top of the glassy carbon electrode over a 500 × 500 nm^2 area (see step height measurement results in the Supplementary materials). Comparing the phase images of the glassy carbon electrodes with (Fig. 6d) and without (Fig. 6c) the coating shows a uniform electropolymerization of PPO on the electrode surface. The surface coverage of the glassy carbon electrode was also studied in a 10 × 10 μ^2 area (see the Supplementary material for further details).

The deposited layer was further characterized using the electrochemical impedance spectroscopy (EIS) method. The magnitude and phase of the impedance for the glassy carbon electrode before and after PPO deposition are shown in Fig. 7. In order to analyze the frequency response of an electrochemical cell, a more complicated model than the one shown in Fig. 1 is required. At very low frequencies, the impedance is under the influence of a non-uniform current distribution [24]. This effect cannot be modeled with a resistor–capacitor (RC) circuit, but a constant phase element can be considered in parallel to the double layer capacitor. The detail of the model and the analysis of the impedance for the full spectrum are provided in the Supplementary materials. However, the impedance of the electrode at higher frequencies can still be modeled with the simplified RC circuit in Fig. 1. Using ZSimpWin software from Princeton Applied Research, the impedance of the electrodes with and without the coating was simulated for frequencies larger than 10 Hz. The simulation results are also shown in Fig. 7. Based on the simulation, the values for C_{eq}, R_P, and R_S are estimated for both electrodes. The values are listed in Table 1.

The result clearly shows that R_P was increased and C_{eq} was decreased after depositing the blocking layer. The series resistance is also reduced after the deposition. The PPO thickness (t_{BL}) can be estimated from the capacitance change. Considering the model in Fig. 2b, the blocking layer capacitance is estimated to be $C_{BL} = 0.8967$ μF based on the measured capacitance ($C_{eq} = 0.7719$ μF) and the double layer capacitance ($C_{DL} = 5.5430$ μF). Since $C_{BL} = \varepsilon_{PPO}A/t_{BL}$ (where ε_{PPO} is the permittivity of PPO – $\varepsilon_{PPO} = 3.5 \times 8.85 \times 10^{-12}$ F m^{-1} [25] – and $A = 0.5$ cm^2 is the surface area of the electrode), the PPO thickness is estimated to be ~1.5 nm. This value is consistent with the previously reported thickness for electrodeposited PPO by other groups [20].

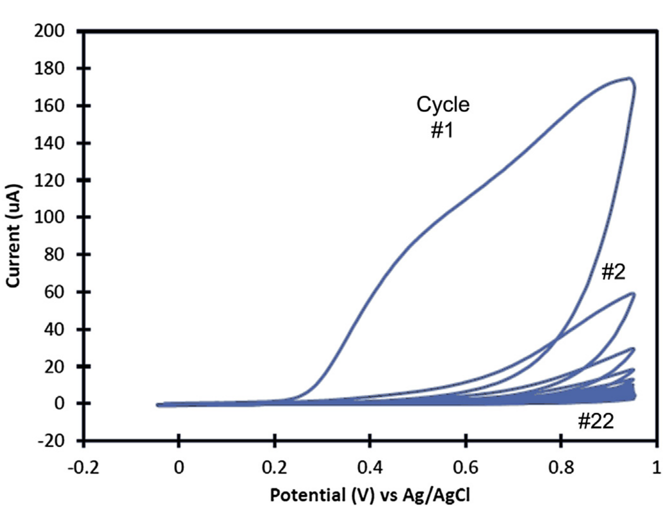

Fig. 5. Electrodeposition of PPO on a glassy carbon electrode using CV method (scan rate 50 mV.s^{-1}); the decrease in the current with subsequent scans indicates the growth of the insulating layer.

3.2. Supercapacitor characterization

In order to study the effect of the blocking layer on the performance of a supercapacitor, two devices were fabricated and tested: one without PPO coating and the other with electrodeposited PPO on both electrodes. The electrode material was activated carbon with high porosity. The polymer was deposited on the electrodes with the same method applied for the glassy carbon electrode (CV with 22 cycles). As expected, the shape of the curves was similar to the one shown in Fig. 5 with much larger current, which was due to the larger surface area of the activated carbon electrode (the result is not presented). The cells were tested at room temperature in a two-electrode configuration using the setup shown in Fig. 4. Various electrochemical experiments were carried out to estimate C_{eq}, R_P, and R_S in both devices.

The nominal voltage in a single cell commercial type supercapacitor is between 2.3 V and 2.75 V [26]. To make a device for that voltage range, chemicals with high level of purity should be utilized and a contaminant-free environment is required for the fabrication [26]. Also, supercapacitors must be sealed before testing. Any contaminant in the electrolyte, especially water/moisture, with the redox potential lower than the nominal voltage would affect the device characteristics. Since our experimental setup has not been designed for the best condition, we tested the cells with the voltages less than 2.0 V to avoid damaging the electrodes. Voltage of 2.0 V is sufficient to supply many low power electronics, including wireless devices [7]. However, in this voltage range, a larger leakage current is expected than an off-the-shelf device. Since the test conditions were the same for both devices with and without the blocking layer, the comparison between the results demonstrates the effect of the blocking layer.

3.2.1. Specific capacitance measurement using cyclic voltammetry

Fig. 8 shows the CV curves in the voltage range of ±2 V across the devices at a scan rate of 50 mV s^{-1}. To obtain the specific current

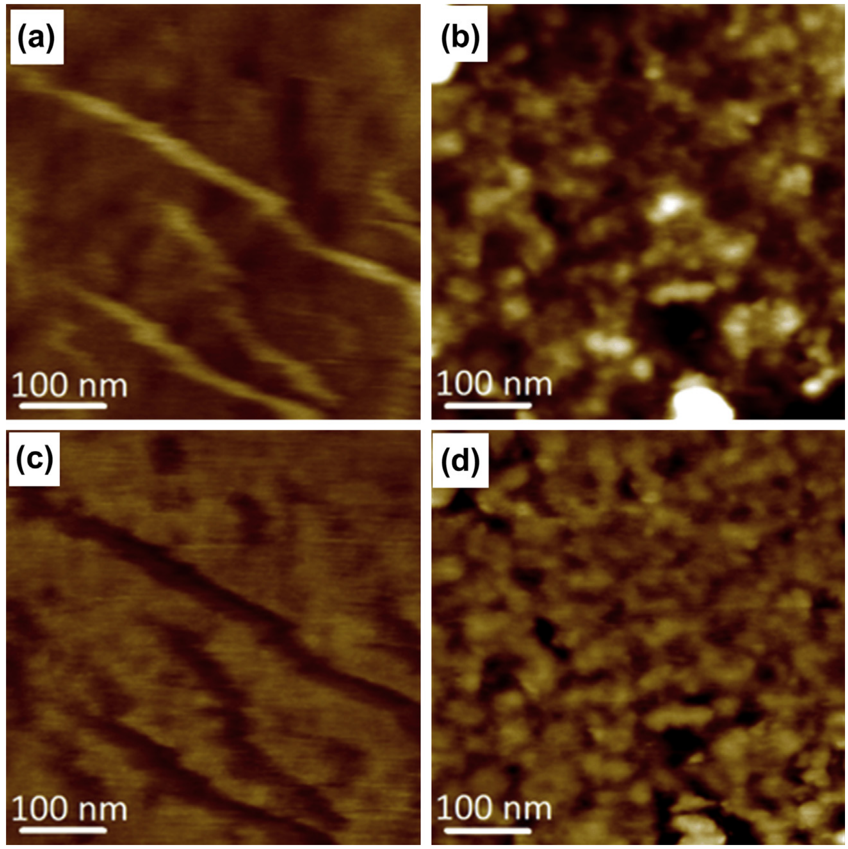

Fig. 6. AFM topographic and phase images of: (a) and (c) uncoated glassy carbon surface and (b) and (d) electro-polymerized PPO on a glassy carbon electrode surface. The images were obtained in air using noncontact tapping mode.

in each cell, the current was normalized to the weight of the activated carbon electrodes. The electrode weight was measured precisely before and after PPO deposition using an analytical balance. The amount of deposited PPO was estimated to be $\sim$7 mg. The PPO deposited electrodes were completely dried before the weight measurement. Since both electrodes are similar, it is expected to have a symmetrical response around 0 V. However, the device with the blocking layer is showing small differences between positive and negative voltages. This is likely due to the different amount of phenol residue in two electrodes of the device.

In a CV measurement, the loop width represents the overall capacitance; and the effect of R_P appears in the slope of the loop [15]. As expected, the loop width is smaller in the device with the PPO coating, which indicates lower specific capacitance. Also, the change in the loop slope implies a lower leakage current for the capacitor with the blocking layer. As a rough approximation (assuming R_S is much smaller than R_P), the specific capacitance can be estimated from half of the ratio of the loop width to the scan rate at zero voltage [15]. Using this method, the cell with the blocking layer had a capacitance of 5.70 F g^{-1} whereas the capacitance of the cell with no coating was 12.99 F g^{-1}, which indicates $\sim$44% reduction in the capacitance after the PPO deposition. In the EIS experiment (Table 1), the capacitance reduced to 14%. The smaller change is likely due to the poor coverage of the PPO layer on the porous activated carbon electrode. In fact, the specific capacitance in the devices with and without the blocking layer implies that the double layer capacitance has to be $\sim$10.16 F g^{-1} (see the model in Fig. 2), while 1.5 nm thickness of the PPO layer suggests specific capacitance of 13.76 F g^{-1}. Hence, the surface coverage is estimated to be $\sim$74% (=10.16/13.76), assuming uniformity in the thickness of PPO on the porous electrode. Considering the weight of the electrodes, C_{eq} was measured to be 0.112 F and 0.0897 F for the devices without and with the blocking layers, respectively.

3.2.2. Leakage current estimation using self-discharge profile

Since R_P changes with voltage, the leakage current estimation from CV is inaccurate. To measure the leakage current at 2.0 V, both cells with and without the blocking layer were first charged for 18 h at 2.0 V. At the end of the time, the charging currents reached to stable values of $\sim$200 μA and $\sim$935 μA for the devices with and without the PPO layers, respectively. These current values are considered as the leakage currents required to maintain the capacitor voltage at 2.0 V [27]. In order to investigate how the leakage current drains the stored energy, the self-discharge profile of the devices was studied. Immediately after the charging, the external voltage source was automatically removed and the open circuit voltage at the cells' terminals was monitored. Fig. 9 shows the self-discharge profiles of the cells with and without the blocking layers. As expected, the blocking layer reduces the leakage current significantly. After 1 h of self-discharge, the cell with the blocking layer displayed a voltage of 1.43 V compared to 1.22 V for the cell without any coating. The leakage current, i_l, was estimated from $i_l = C_{eq}\, dV/dt$ (at $t = 0$) where dV/dt is the slope of the self-discharge profile at $t = 0$. The leakage currents in the devices with and without the blocking layer are estimated to be 220 μA and 996 μA, respectively. These values are close to the measured currents at the end of the 18 h charging cycle. Knowing the leakage current, the R_P values at 2 V were obtained from Ohm's law. The resistance values and other parameters in supercapacitors are listed in Table 2.

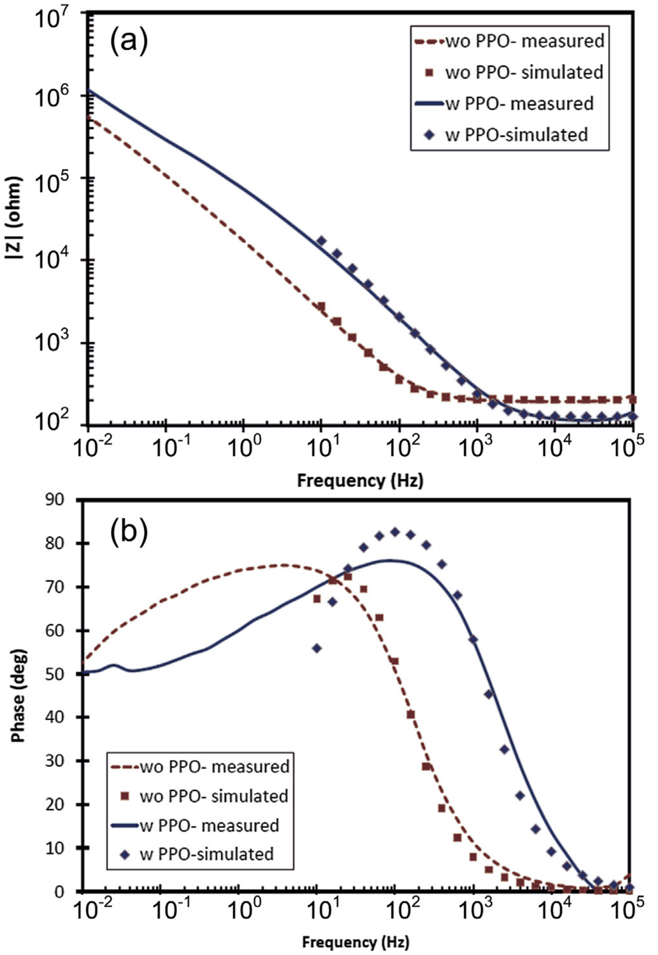

Fig. 7. (a) Magnitude and (b) phase of the measured and simulated impedance for the glassy carbon electrodes with and without the PPO layer. Simulations were performed based on the model in Fig. 1 for frequencies between 10 Hz and 100 kHz. A more complicated model has been discussed in the Supplementary materials section which explains the behavior of the cells for the entire spectrum.

It should be noted that the leakage current estimation with this method requires a long charging time (i.e. 18 h) to assure the diffusion of ions into deep nanopores on the electrodes [8]. In a short charging time, only the double layer capacitors at shallow pores are charged. Switching to the open circuit mode, a voltage drop occurs due to the redistribution of charges between shallow and deep pores [8]. This effect is different from the leakage current produced by Faradic reactions at the electrode surfaces.

3.2.3. R_S measurement using galvanic pulses

Galvanostatic charging/discharging is a common method for R_S measurement. In this study, ±1 mA current pulses (period of 200 s) were applied to charge and discharge the supercapacitors and the voltage across the devices was monitored (Fig. 10). The voltage drop at the charge/discharge transition divided by the current difference

Table 1
Simulated values for C_{eq}, R_P, and R_S in the glassy carbon electrode with and without the PPO coating. The measured data was obtained from EIS.

Characteristics	Without blocking layer	With blocking layer
C_{eq} [μF]	5.5430	0.7719
R_P [kΩ]	8.49	30.9
R_S [Ω]	207	128

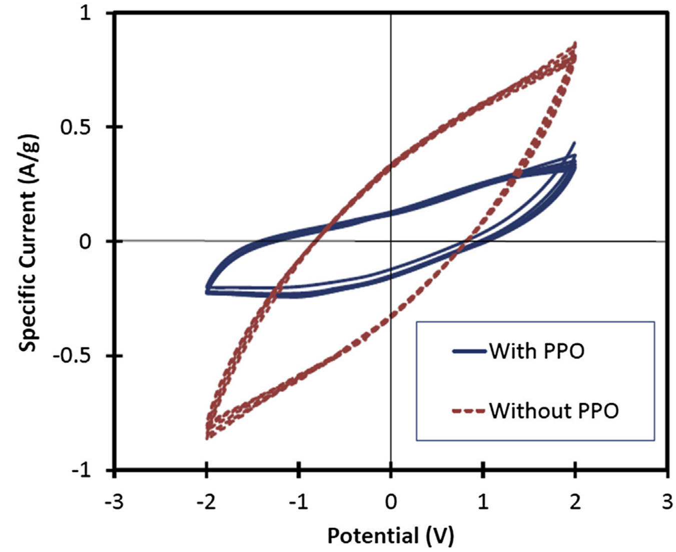

Fig. 8. Cyclic voltammograms for two supercapacitors: with and without the PPO blocking layer. The scan rate was 50 mV s^{-1}.

(2 mA) gives the R_S value (Table 2). The higher resistance in the device with the PPO layer is likely due to the increased series resistance between the activated carbon and the current collector (glassy carbon). For practical applications, a very low series resistance (less than 1 Ω) is required. The devices presented in this work were not optimized for low series resistance. The large observed resistances in both devices are mainly due to the mechanical contacts between the activated carbon electrode and the glassy carbon. To eliminate this problem, activated carbon electrodes with laminated current collector are recommended for future works.

As shown in Fig. 10, the voltage increases with time when a supercapacitor is charged with a constant current. A small voltage change, ΔV, is expected for a large capacitor. A ΔV of about 2 V was observed in the capacitor with the blocking layer, while the voltage change was only 0.8 V in the device without any coating. This again confirms the reduction of specific capacitance as the result of the blocking layer.

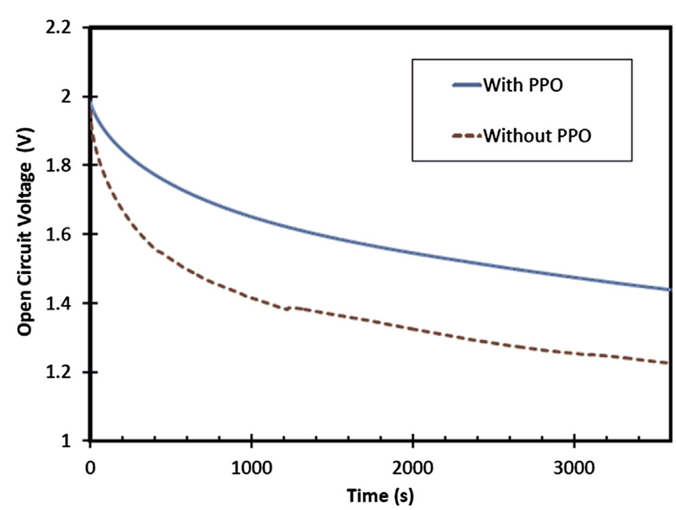

Fig. 9. Self-discharge profile in two supercapacitors with and without the blocking layer. Both capacitors were charged at 2.0 V for 18 h prior to open circuit voltage measurement.

Table 2
The characteristics of the supercapacitors without and with the blocking layer.

Characteristics	Without blocking layer	With blocking layer
Specific capacitance [F g^{-1}]	12.99	5.70
Leakage current (at 2.0 V) [μA]	996	220
C_{eq} [F]	0.112	0.0897
R_P (at 2.0 V) [kΩ]	1.97	9.05
R_S [Ω]	66	194
Voltage (at $t = 0$ s) [V]	2.0	2.0
Voltage (at $t = 3600$ s) [V]	1.23	1.44
Specific energy (at $t = 0$ s) [J g^{-1}]	25.98	11.40
Specific energy (at $t = 3600$ s) [J g^{-1}]	9.76	5.90
Specific energy loss in 1 h [J g^{-1}].	16.22	5.50

4. Discussion

As shown in Table 2, the application of the blocking layer has reduced the supercapacitor's leakage current by 78%. However, the specific capacitance was decreased from 12.99 F g^{-1} to 5.70 F g^{-1}. As a result, the specific energy, also known as energy density ($C_{sp}V^2/2$), of the supercapacitor with the blocking layer was lower than that in the device without any coating by about 56% at the charging voltage of 2.0 V. As shown in Fig. 9, the open circuit voltage of the capacitor without the coating dropped from 2.0 V to 1.23 V in 1 h, whereas the voltage change in the device with the blocking layer was only 0.56 V in the same period. Therefore, the amounts of the stored energy density after 1 h of self-discharge were 5.90 J g^{-1} and 9.76 J g^{-1} for devices with and without the PPO layer, respectively. The lower energy loss implies that the energy storage efficiency is improved by the application of the blocking layer. It should be noted that the energy loss and leakage current in the devices presented in this work are higher than those values in a typical supercapacitor on the market. This is mainly due to contaminants (e.g. water) in the electrolyte of the devices fabricated in our lab. To avoid contamination, it is recommended to use electrolyte with high purity and do the fabrication and test in a glove box. Nevertheless, the studied approach in this work demonstrates the feasibility of reducing leakage current in any electrolytic double layer capacitor by application of a thin blocking layer.

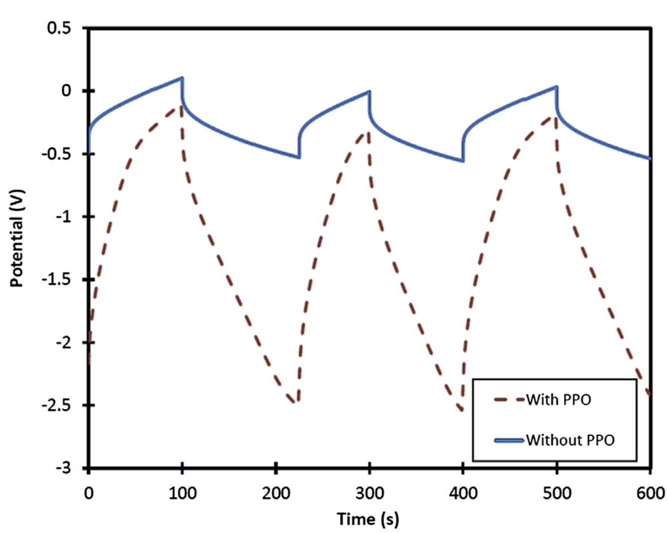

Fig. 10. Galvanic pulses for measuring series resistance in supercapacitors with and without PPO layer. Current pulses of ±1 mA with 200 s period were applied to charge and discharge the devices. The voltage drop at the transition from +1 mA to −1 mA was measured. The resistance was calculated from the voltage difference divided by the 2 mA current difference.

The energy storage density could be improved if a thinner blocking layer were used. Of course the leakage current would be higher with a thinner PPO layer. Further study is required to investigate the effect of the blocking layer thickness on the specific capacitance, energy density, and leakage current in a device. Due to the self-terminating effect in the electropolymerization of PPO, it is difficult to control the thickness of the deposited layer. A cyclic voltammetry with a fewer number of cycles may produce thinner films, but the layer would likely have defects. Other methods such as atomic layer deposition (ALD) has been planned to be employed for depositing an ultrathin film of an insulator (e.g. Al_2O_3 and Barium Strontium Titanate-BST). The thickness of the layer can be well controlled by using ALD. Also, different insulating materials can be tested.

5. Conclusions

As a solution for reducing the leakage current in supercapacitors, application of an ultra-thin blocking layer has been demonstrated. The experimental results from a 1.5 nm thick layer of PPO on activated carbon electrodes of a supercapacitor show that the leakage current was reduced by 78%. However, the specific capacitance and the energy storage density were decreased by 56%. Due to the lower leakage current, the amount of energy waste was significantly lower in the device with the blocking layer, compared to the device with no coating. In conclusion, deposition of the blocking layer can be used to make more efficient supercapacitors for the applications which need longer charge storage time. More study on the thickness and material of the blocking layer is required to optimize the performance of supercapacitors with the blocking layer.

Appendix A. Supplementary material

Supplementary data related to this article can be found at http://dx.doi.org/10.1016/j.jpowsour.2013.04.150.

References

[1] M. Winter, R.J. Brodd, Chemical Reviews 104 (2004) 4245–4270.
[2] P. Simon, Y. Gogotsi, Nature Materials 7 (2008) 845–854.
[3] A. Burke, Journal of Power Sources 91 (2000) 37–50.
[4] G. Park, T. Rosing, M. Todd, C. Farrar, W. Hodgkiss, Journal of Infrastructure Systems 14 (2008) 64–79.
[5] X. Jiang, J. Polastre, D. Culler, in: Fourth International Symposium on Information Processing in Sensor Networks, 2005, pp. 463–468.
[6] V.V.N. Obreja, Physica E Low-dimensional Systems and Nanostructures 40 (2008) 2596–2605.
[7] V.C. Gungor, G.P. Hancke, IEEE Transactions on Industrial Electronics 56 (2009) 4258–4265.
[8] H. Yang, Y. Zhang, Journal of Power Sources 196 (2011) 8866–8873.
[9] F. Belhachemi, S. Rael, B. Davat, IEEE Industry Applications Conference (2000) 3069–3076.
[10] D. Petreus, D. Moga, R. Galatus, R.A. Munteanu, Advances in Electrical and Computer Engineering 8 (2008) 15–22.
[11] Y. Diab, P. Venet, H. Gualous, G. Rojat, IEEE Transactions on Power Electronics 24 (2009) 510–517.
[12] J. Niu, B.E. Conway, W.G. Pell, Journal of Power Sources 135 (2004) 332–343.
[13] B.E. Conway, W.G. Pell, T.C. Liu, Journal of Power Sources 65 (1997) 53–59.
[14] B.W. Ricketts, C. Ton-That, Journal of Power Sources 89 (2000) 64–69.
[15] A.J. Bard, L.R. Faulkner, Electrochemical Methods Fundamentals and Applications, second ed., John Wiley, New York, 2001.
[16] CAP-XX, Application Note AN1005 Rev 2.2, Simple Measurement of Supercapacitor Parameters (2009).
[17] P. Mars, How Supercapacitors Solve LED Flash Power Issues in High Res Camera Phones, EE Times Design (2006).
[18] G. Injeti, B. Leo, Science and Technology of Advanced Materials 9 (2008) 043001.
[19] C.P. Rhodes, J.W. Long, M.S. Doescher, J.J. Fontanella, D.R. Rolison, The Journal of Physical Chemistry B 108 (2004) 13079–13087.
[20] R.L. McCarley, R.E. Thomas, E.A. Irene, R.W. Murray, Journal of Electroanalytical Chemistry and Interfacial Electrochemistry 290 (1990) 79–92.
[21] R.L. Mccarley, E.A. Irene, R.W. Murray, Journal of Physical Chemistry US 95 (1991) 2492–2498.

[22] C.P. Rhodes, J.W. Long, M.S. Doescher, B.M. Dening, D.R. Rolison, Journal of Non-Crystalline Solids 350 (2004) 73–79.
[23] J. Kang, H. Li, S. Cushing, J. Wang, N. Wu, ECS Transactions 19 (2009) 159–164.
[24] M. Paunovic, M. Schlesinger, Fundamentals of Electrochemical Deposition, second ed., Wiley & Sons, Hoboken, NJ, 2006.
[25] D. Ionescu, I.B. Ciobanu, Romanian Reports in Physics 61 (2009) 676–688.
[26] A. Izadi-Najafabadi, MS Thesis in Electrical and Computer Engineering, University of British Columbia, 2006.
[27] http://avt.inel.gov/battery/pdf/FreedomCAR_Capacitor_Test_Manual_Sept_2004.pdf.